Insights into Cytochrome *c*−Cardiolipin Interaction. Role Played by Ionic Strength[†]

Federica Sinibaldi,[‡] Laura Fiorucci,[‡] Antonella Patriarca,[‡] Rosaria Lauceri,[§] Tommaso Ferri,[||] Massimo Coletta,[‡] and Roberto Santucci*[,‡]

Dipartimento di Medicina Sperimentale e Scienze Biochimiche, Università di Roma "Tor Vergata", 00133 Roma, Italy, Dipartimento di Scienze Chimiche, Università di Catania, 95100 Catania, Italy, and Dipartimento di Chimica, Università di Roma "La Sapienza", 00185 Roma, Italy

Received January 9, 2008; Revised Manuscript Received April 22, 2008

ABSTRACT: The finding that cytochrome *c* (cyt *c*) plays a role in programmed cell death after its release from the mitochondrion has recently renewed interest in this protein. The structural changes in cytochrome *c* observed at early stages of the apoptotic process have been related to changes occurring in the protein when it forms a complex with phospholipid vesicles. Among the lipids constituting the membrane, cardiolipin is the one thought to bind to cyt *c*. In this paper, we have investigated the influence exerted by ionic strength on cytochrome *c*−cardiolipin interaction and found that formation of the cytochrome *c*−cardiolipin complex occurs via two distinct transitions, implying a high-affinity site and a low-affinity site. Ionic strength significantly influences complex stability; sodium chloride dissociates the complex through two distinct transitions, the second of which occurs at a very high anion concentration. ATP also dissociates the complex, but under the conditions that were investigated, its action is limited to the high-affinity site. The dissociation process is characterized by a very slow kinetic rate constant ($k_{obs} = 4.2 \times 10^{-3}$ s^{-1}) and requires several minutes to be completed. We ascribe it to the high activation barrier met by the protein when restoring the native Fe(III)−M80 axial bond. The peroxidase activity shown by cardiolipin-bound cytochrome *c* is indicative of a less packed protein tertiary conformation in the complex. In line with earlier reports, these data highlight the manifold functions of cytochrome *c* besides the well-known role it plays in oxidative phosphorylation, shedding more light on the properties of the cytochrome *c*−cardiolipin complex, involved in the progression of early stages of apoptosis.

Cytochrome *c* (cyt *c*)[1] is a single-chain hemoprotein composed of 104 amino acids, acting as an electron carrier in mitochondria. It contains the heme as a prosthetic group lying within a crevice and covalently attached to the polypeptide chain by two thioether bridges formed with residues C14 and C17. H18 and M80 are the axial ligands of the heme iron in the native protein (*1*). As a mitochondrial peripheral membrane protein, cyt *c* functions between the inner and outer membrane, mediating electron transfer between different proteins of the respiratory chain; more specifically, cyt *c* mediates electron transfer between cyt *c* reductase and cyt *c* oxidase (*2–4*).

The finding that cyt *c* plays a role in programmed cell death (i.e., in cell apoptosis) after its release from the mitochondrion has recently renewed interest in this protein (*5, 6*). In the cytoplasm, cyt *c* binds to the apoptosis protease activation factor (APAf-1) and forms a complex which, activating pro-caspase 9, gives rise to an enzymatic reaction cascade leading to apoptosis in cells (*7–9*). The structural changes involving cyt *c* in cell apoptosis have been related to changes occurring in the protein when it forms a complex with phospholipid vesicles at an early stage of the process (*3, 10*). Among the lipids constituting the membrane, cardiolipin (CL), a phospholipid with two negatively charged phosphate groups and four fatty acyl chains, is that appointed to bind to cyt *c* (*11–13*). The interaction between cyt *c* and CL induces changes in the protein tertiary structure, including perturbation of the heme pocket region and displacement of Met80 from the sixth coordination position of the heme iron. As recently observed, the less packed non-native conformation assumed by the protein in the complex formed with CL facilitates the access of small molecules, such as hydrogen peroxide, to the heme site (*14*). The peroxidase activity acquired by phospholipid-bound cyt *c* turns out to be critical in the early stages of apoptosis; acting as a powerful CL-specific peroxidase, the complex generates CL hydroperoxides which actively contribute to the release of protein from the mitochondrial membrane (*15, 16*).

Studies on cyt *c*−phospholipid interactions have revealed the presence, on the protein, of (at least) two binding sites for CL, named the A-site and the C-site (*17, 18*). At the A-site, which is thought to be composed of a network of positively charged residues (possibly K72, K73, and K86), the interaction of the protein with CL is electrostatic in nature and involves the deprotonated (negatively charged) phospholipid. The protein−CL interaction at the C-site, on the

[†] This research was funded in part by grants from Italian Ministry for University and Research (MIUR FIRB RBNE03PX83 to M.C.).

* To whom correspondence should be addressed: Dipartimento di Medicina Sperimentale e Scienze Biochimiche, Università di Roma "Tor Vergata", Via Montpellier 1, 00133 Roma, Italy. Phone: +39 06 72596364. Fax: +39 06 72596353. E-mail: santucci@med.uniroma2.it.

[‡] Università di Roma "Tor Vergata".

[§] Università di Catania.

[||] Università di Roma "La Sapienza".

[1] Abbreviations: cyt *c*, cytochrome *c*; CL, cardiolipin; CD, circular dichroism; GdmHCl, guanidinium hydrochloride.

10.1021/bi800048v CCC: $40.75
Published on Web 06/10/2008

other hand, is hydrophobic in nature, stabilized by H-bonding between residue N52 of cyt *c* and protonated CL. According to the so-called extended lipid conformation hypothesis (*19*), one acyl chain of the phospholipid accommodates to a hydrophobic channel of the protein which extends from the surface to the heme pocket region, while the other chain points in the opposite direction from the headgroup. The pH affects the cyt *c*−CL interaction; at low pH, the cyt *c*−CL complex forms via the C-site of the protein (acidic environment favors CL protonation), while at neutral pH, cyt *c* binds to CL via both the A-site and the C-site (*12, 18*). Around neutrality, ionic strength influences the cyt *c*−CL interaction; the cyt *c*−CL complex spontaneously forms at low ionic strength and undergoes dissociation at high ionic strength (*17, 18*). An additional binding site for phospholipids, indicated as the L-site, was recently detected at acidic pH. Like the A-site, the L-site is electrostatic in nature, being composed of a cluster of positively charged residues (possibly K22, K27, and H33) (*20*).

To gain deeper insight into the influence exerted by the ionic strength on the cyt *c*−CL interaction, the binding of CL to cyt *c* has been investigated kinetically and at equilibrium. Results we obtained provide new information about the role played by ionic strength in influencing cyt *c*−CL binding and complex stability around neutrality.

MATERIALS AND METHODS

Materials. Horse heart cyt *c* (type VI, oxidized form) and bovine heart cardiolipin (>80% polyunsatured fatty acid content, primary linoleic acid; 98% purity) were from Sigma Chemical Co. (St. Louis, MO) and were used without further purification. All reagents were analytical grade.

Circular Dichroism Measurements. Circular dichroism (CD) measurements were carried out using a Jasco (Tokyo, Japan) J-710 spectropolarimeter equipped with a personal computer as a data processor. The molar ellipticity, (θ) (degrees square centimeter per decimole), is expressed on a molar heme basis in the Soret (400−450 nm) region. In the far-UV region, measurements (not shown) were carried out in the 215−250 nm range.

Binding of cyt *c* to CL vesicles [cmc of approximately 1 μM, as determined by the spectroscopic method based on the fluorescence of 1,6-diphenylhexatriene (*21*)] was investigated by following the changes induced in the Soret CD spectrum (400−450 nm) of the protein by stepwise addition of few microliters of a 3.5 mM CL ethanol solution to a 10 μM cyt *c* solution (V_i = 1 mL; 0.5 cm path length cell). The buffer consisted of 25 mM Hepes and 0.1 mM EDTA (pH 7.0). Dichroic spectra were recorded after the sample had been mixed for 5 min. The same procedure was employed to follow the salt-induced dissociation of the complex (cyt *c*−CL).

Electronic Absorption Measurements. Electronic absorption measurements were carried out at 25 °C using a Jasco V-530 spectrophotometer. An extinction coefficient (ε_{408}) of 106 mM^{-1} cm^{-1} was used to determine the cyt *c* concentration.

Fast Kinetics Measurements. Kinetic measurements were carried out employing either (i) a rapid-mixing stopped-flow apparatus (Biologic SAS, Claix, France) with a dead time of 10 ms, interfaced with a Jasco J-710 spectropolarimeter (for CD kinetics), or (ii) a rapid-mixing stopped-flow SX.18 MV apparatus (Applied Photophysics Co., Salisbury, U.K.) with a dead time of 1 ms, equipped with a diode array for collection of transient spectra over the 350−700 nm absorption range (for absorption kinetics).

For CD kinetics, ferric cyt *c* was mixed with CL (at pH 7.0) and progress curves were followed at 416 nm, with a 0.2 cm path length observation cell. In the case of absorption kinetics, the diode array allowed collection of transient spectra with a 1 ms time resolution. From these, it was also possible to collect progress curves at individual wavelengths as well as absorption spectra at given time intervals. The same procedure was used to follow the NaCl-induced complex dissociation.

Kinetic progress curves were fitted according to the following equation:

$$S_{obs} = S_\infty \pm \sum_{i=1}^{i=n} \Delta S_i \, e^{(-k_i t)} \quad (1)$$

where S_{obs} is the signal (via either circular dichroism or absorption) at a given wavelength and at a given time interval, S_∞ is the signal (via either CD or absorption) at longer time intervals (when the reaction is completed), ΔS_i is the signal change for phase *i*, k_i is the rate constant for phase *i*, and *t* is time. The ± sign means that, at different wavelengths, the signal intensity may either decrease or increase.

Peroxidase Activity Measurements. The peroxidase activity of cyt *c* and of the cyt *c*−CL complex (at varying CL concentrations) was measured at pH 7.0 and 25 °C using 1 mM hydrogen peroxide and 10 mM guaiacol. Product formation (tetraguaiacol; ε_{470} = 26.6 mM^{-1} cm^{-1}) was followed using a Jasco V-530 spectrophotometer. The protein concentration was 1 μM. The same experiments were carried out by using GdmHCl (at concentration varying within the 0−6 M range) in place of CL. Data were reported as fractions of the "plateau" value.

RESULTS

Cyt c Binding to CL. For hemoproteins, the Soret CD spectrum is strictly correlated with the heme pocket conformation (*22*). In particular, the negative 416 nm Cotton effect is considered diagnostic of Fe(III)−M80 coordination in native cyt *c* (*23, 24*); changes in the 416 nm dichroic signal reveal alterations of the heme pocket region which involve the displacement of M80 from the axial coordination to the heme iron (*24, 25*) and a rearrangement of the tertiary structure with formation of non-native compact forms of the polypeptide [as the molten globule (*25*)] or, in some cases, of the unfolded state. A CD investigation of the cyt *c*−CL interaction is particularly interesting for two main reasons. (i) As described above, the heme pocket alteration is rapidly detected by the 416 nm dichroic band; (ii) the binding process cannot be successfully followed by absorbance spectroscopy because the optical spectrum of the cyt *c*−CL complex is very similar to that of free cyt *c* (spectra not shown). Figure 1 illustrates the Soret CD spectrum of cyt *c* at pH 7.0, in the absence and presence of CL (CL:cyt *c* molar ratio of 6:1). The disappearance of the negative 416 nm Cotton effect observed upon addition of CL in solution provides clear evidence that the polyphosphate induces consistent alteration of the protein heme pocket region. Absorbance measurements

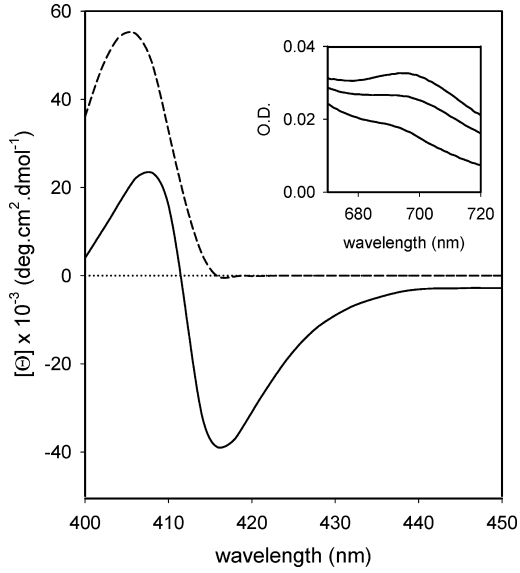

FIGURE 1: CL binding to cyt *c*. Soret CD spectrum of cyt *c* recorded in the absence (—) and presence (– – –) of 60 μM CL. The protein concentration was 10 μM. Experimental conditions: 25 mM Hepes and 0.1 mM EDTA (pH 7.0). The temperature was 25 °C. The inset shows the absorbance spectrum of cyt *c* in (from top to bottom) the absence and presence of 25 and 60 μM CL. The wavelength range was 670−720 nm.

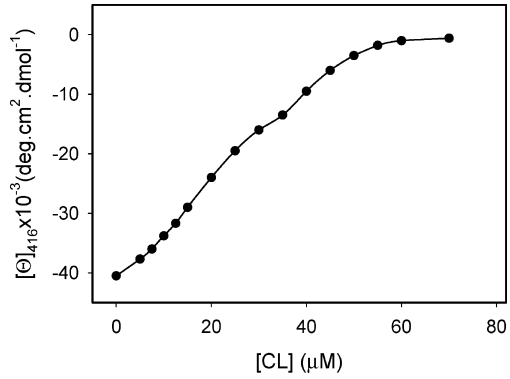

FIGURE 2: Titration curve for CL binding to cyt *c*. Changes in the 416 nm Cotton effect induced by stepwise addition of CL to a 10 μM cyt *c* solution. Experimental points are averages of at least three measurements. Other conditions were as described in the legend of Figure 1.

carried out in the 670−720 nm range, shown in the inset of Figure 1, confirm displacement of M80 from the sixth coordination position of the heme iron. As shown in Figure 2, the stepwise addition of CL in solution brings about two distinct transitions leading to formation of the cyt *c*−CL complex. This observation suggests that the protein binds to CL via (at least) two distinct binding sites characterized by different affinities for the phospholipid. Since the two-transition process suggests that the two binding sites are functionally independent, analysis of data was carried out according to the following equation:

$$Y = \alpha\frac{(K_1[\mathrm{L}])^n}{1+(K_1[\mathrm{L}])^n} + (1-\alpha)\frac{(K_2[\mathrm{L}])^m}{1+(K_2[\mathrm{L}])^m} \qquad (2)$$

where K_1 and K_2 are the affinity constants for the two binding sites, [L] is the free ligand concentration (i.e., CL concentration for data depicted in Figure 2 and NaCl concentration for data depicted in Figure 3), n and m are the cooperativity

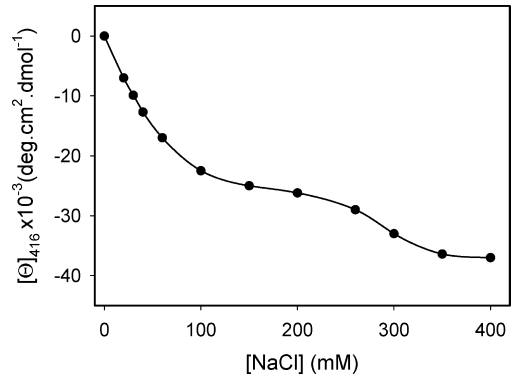

FIGURE 3: NaCl-induced dissociation of the cyt *c*−CL complex. Changes in the 416 nm Cotton effect induced by stepwise addition of NaCl to a 10 μM cyt *c* solution containing 60 μM CL. Experimental points are averages of at least three measurements. Other conditions were as described in the legend of Figure 1.

indexes for the high-affinity and low-affinity sites, respectively, and α is the relative spectral contribution for CL binding to the high-affinity site. Equation 2 is a phenomenological equation reflecting a process characterized by two transitions with cooperative binding behavior. From analysis of data, a K_1 of $(4.9 \pm 0.5) \times 10^4$ M^{-1} for the first transition ($n = 2.0 \pm 0.3$) and a K_2 of $(2.4 \pm 0.5) \times 10^4$ M^{-1} for the second transition ($m = 4.0 \pm 1.0$) were determined. Further, the value of the spectral contribution to the Cotton effect that was determined ($\alpha = 0.78 \pm 0.08$) turns out to be much larger for the high-affinity site. As a whole, data obtained suggest the presence of a larger number of high-affinity sites than low-affinity sites; from a functional viewpoint, the latter sites appear to be more tightly correlated, displaying a higher degree of cooperativity.

The shape of the graph of Figure 2 reveals that both sites must be saturated to achieve full protein population bound to CL (corresponding, at CD, to the full disappearance of the negative 416 nm Cotton effect). Any hypothesis of protein denaturation is excluded since the α-helix content of CL-bound cyt *c* is comparable to that of the free protein [as revealed by the far-UV CD spectrum (not shown)]. The observation that cyt *c*−CL binding is characterized by two distinct transitions is in good accord with previous hypothesis claiming the existence on the protein of two distinct binding sites for CL, named the A-site and the C-site (*17, 18*).

Measurements carried out as a function of pH [pH range of 6.5−7.5 (not shown)] do not highlight significant differences in the protein−CL binding process. However, while at pH 6.5 turbidity is observed in solution in the presence of 60 μM CL, at pH 7.5 it becomes visible at 80 μM CL. We noted that turbidity significantly alters the Soret CD spectrum, the 408 nm Cotton effect becoming stronger and differently shaped (not shown).

Salt-Induced Complex Dissociation. The increase in ionic strength due to addition of sodium chloride in solution affects the cyt *c*−CL binding reaction. Data depicted in Figure 3 provide clear evidence that the salt induces dissociation of the cyt *c*−CL complex (at 0.4 M salt the negative 416 nm dichroic signal, typical of the free protein, is almost fully recovered), indicating that at neutrality the complex stability is modulated by ionic strength. In agreement with the data depicted in Figure 2, the two-transition profile of Figure 3 is consistent with the presence on the protein of two distinct

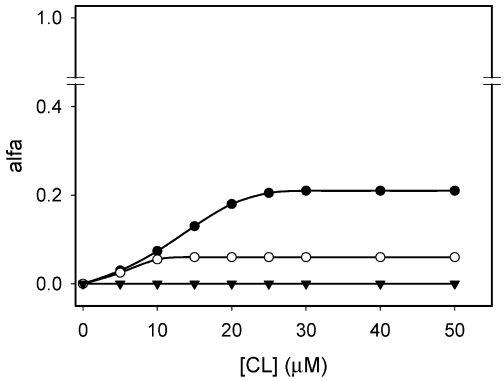

FIGURE 4: Effect of ionic strength on the formation of the CL−cyt c complex. Changes in the 416 nm dichroic signal induced by addition of CL to a 10 μM cyt c solution, in the presence of (●) 0.1, (○) 0.12, and (▼) 0.2 M sodium chloride. alfa indicates the fraction of protein molecules interacting with CL. The 416 nm ellipticity values of the spectra of Figure 1 were taken as end points of the binding transition. Experimental points are averages of at least three measurements. Other conditions were as described in the legend of Figure 1.

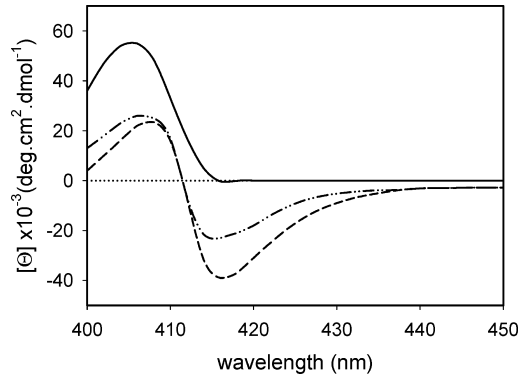

FIGURE 5: ATP-induced CL−cyt c complex dissociation. Changes induced by ATP on the Soret CD spectrum of cyt c in the presence of 55 μM CL: cyt c with CL (—) and cyt c with CL in the presence of 15 mM ATP (—·—). The CD spectrum of native cyt c (———) is shown for comparative purposes. Other conditions were as described in the legend of Figure 1.

binding sites for CL which are differently influenced by ionic strength. Analysis of the NaCl-induced dissociation of the cyt c−CL complex was performed according to eq 2, in which it is assumed that dissociation of the complex results from a competitive action of the salt for binding to the protein. A K_1 of $(2.1 \pm 0.3) \times 10^4$ M^{-1} was determined for the first transition ($n = 1.0 \pm 0.3$). For what concerns the second transition, the limited number of experimental points renders the evaluation of m uncertain; indicatively, a K_2 of $(3.4 \pm 0.6) \times 10^3$ M^{-1} is determined for an m of 3.0 ± 1. The value of the spectral contribution ($\alpha = 0.78 \pm 0.08$) is identical to that determined above for CL binding to the protein. As a whole, data suggest that the high-affinity site for CL is also the site more sensitive to the presence of salt in solution.

Earlier work (*17, 18*) proposed a competitive action of anions versus deprotonated CL at a level of the A-site to explain the salt-induced dissociation of the cyt c−CL complex. To gain deeper insight into this point, we investigated the cyt c−CL interaction as a function of ionic strength. Thus, CL was added to protein solutions containing different salt concentrations. The profiles in Figure 4, obtained at 0.1, 0.12, and 0.2 M NaCl, provide clear evidence of the role played by electrostatics in the binding process: while at 0.1 M salt approximately 20% of the protein interacts with CL, at 0.12 M salt the percentage drops to approximately 10%, and no binding is monitored in the presence of 0.2 M salt.

ATP-Induced Complex Dissociation. Previous work (*26*) formulated the hypothesis that the cyt c−phospholipid interaction is influenced by ATP only at the level of the A-site. To shed more light on this point, CD measurements were carried out on the protein in the presence of 55 μM CL. Under these conditions, approximately 100% of the protein is bound to the phospholipid via both the high-affinity and low-affinity sites (see Figure 1). We found that ATP affects the dichroic signal; addition of increasing amounts of ATP in solution, to a concentration of ≤10 mM, gradually increases the strength of the negative 416 nm Cotton effect. Then the CD spectrum remains unchanged between 10 and 15 mM ATP. Figure 5 shows the Soret CD spectrum recorded in the presence of 15 mM ATP; the nucleotide increases the strength of the negative 416 nm Cotton effect to approximately one-half of that of the native protein. This indicates that approximately 50% of the complex undergoes dissociation; interestingly, this is the amount of protein estimated to be bound to CL via the high-affinity site (see Figure 2). This suggests that, under the conditions investigated, ATP competes with CL for one of the two protein binding sites only, namely, that exhibiting a high affinity for polyphosphates. We found that ATP concentrations of >15 mM cause turbidity in solution; therefore, it was not possible to determine if, like sodium chloride, ATP at a higher concentration also competes with CL for the low-affinity binding site.

Kinetics of Cyt c−CL Binding and Dissociation. CL binding to cyt c does not produce significant changes in the absorption spectrum of the protein. However, we were able to investigate the cyt c−CL binding kinetics at 695 nm by following the effect of CL on the CT absorption band of cyt c [considered a diagnostic indicator of the integrity of the Met80−Fe(III) bond (*24*)]. As shown in Figure 6, the kinetics is characterized by a decrease in absorption, ascribed to the rupture of the Fe−Met80 axial bond. We found that the curve amplitude increases with the CL:cyt c molar ratio. The observed rate constant is independent of the CL concentration ($k_{obs} = 1.83 \pm 0.29$ s^{-1}), which suggests the existence of a rate-limiting step represented, perhaps, by the Fe−Met80 bond cleavage.

More relevant signal change is achieved by CD. In this case, we followed the CL-induced changes in the 416 nm Cotton effect. Figure 7 shows the progress curves obtained at 15, 40, and 70 μM CL. CL influences (i.e., decreases) the intensity of the negative dichroic band as a function of its concentration: the higher the CL:cyt c molar ratio, the greater (i) the change in the magnitude of the signal and (ii) the amplitude of the kinetic curves. The observed rate constant ($k_{obs} = 1.83 \pm 0.19$ s^{-1}) is virtually identical to that determined by absorption at 695 nm and, also in this case, independent of CL concentration. Unfortunately, the low signal-to-noise ratio of progress curves does not allow a detailed description of the steps characterizing the cooperative interaction at equilibrium (Figure 2). Even though the binding process is likely to be more complex, here we illustrate the simplest reaction scheme that may account for

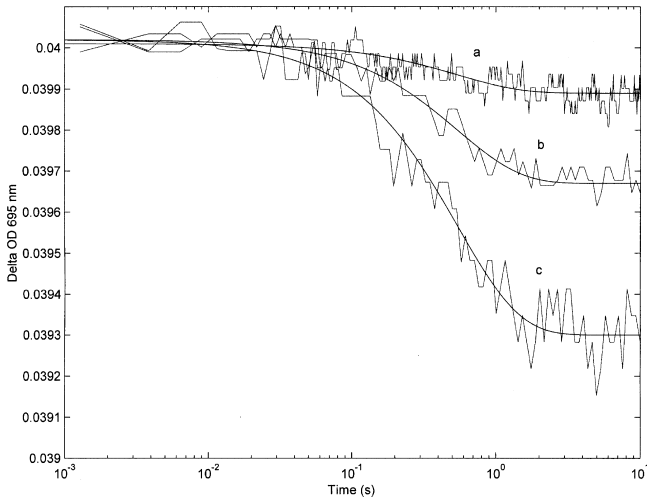

FIGURE 6: Kinetics of CL binding to cyt *c*, followed by absorption at 695 nm. Kinetic progress curves: 50 μM cyt *c* mixed with 80 μM CL (a), 50 μM cyt *c* mixed with 160 μM CL (b), and 50 μM cyt *c* mixed with 250 μM CL (c). Solid lines correspond to nonlinear least-squares fitting of data to eq 1, employing the following values: (a) $S_\infty = 0.0399$, $\Delta S = 0.00012$, and $k = 1.83$ s^{-1}, (b) $S_\infty = 0.0397$, $\Delta S = 0.00035$, and $k = 1.83$ s^{-1}, and (c) $S_\infty = 0.0394$, $\Delta S = 0.00072$, and $k = 1.83$ s^{-1}. The curves shown are averages of five accumulations, to improve the signal-to-noise ratio. The temperature was 20 °C.

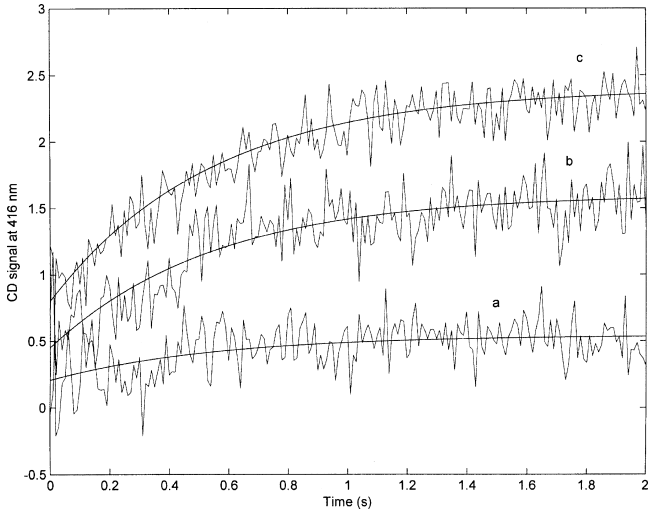

FIGURE 7: Kinetics of CL binding to cyt *c*, followed by CD at 416 nm. Kinetic progress curves: 5 μM cyt *c* mixed with 15 μM CL (a), 5 μM cyt *c* mixed with 40 μM CL (b), and 5 μM cyt *c* mixed with 70 μM CL (c). Solid lines correspond to nonlinear least-squares fitting of data to eq 1, employing the following values: (a) $S_\infty = 0.54$, $\Delta S = 0.33$, and $k = 1.83$ s^{-1}, (b) $S_\infty = 1.59$, $\Delta S = 1.15$, and $k = 1.83$ s^{-1}, and (c) $S_\infty = 2.38$, $\Delta S = 1.62$, and $k = 1.83$ s^{-1}. Progress curves b and c have been displaced by 0.15 and 0.4 unit, respectively, for the sake of clarity. The curves shown are averages of eight accumulations, to improve the signal-to-noise ratio. The temperature was 20 °C.

kinetic data obtained, where the first step of the process (characterized by a cleavage rate constant k_{+1} and a backward rate constant k_{-1}) consists of cleavage of the axial Fe−Met80 bond, while the successive step (characterized by a bimolecular binding rate constant k_{+2} and a dissociation rate constant k_{-2}) consists in the first step of binding of CL to cyt *c*. Clearly, the latter process is a phenomenological representation of a more complex, multistep cooperative mechanism which, at present, cannot be better determined.

Scheme 1

$$\text{Fe-Met80 + CL} \underset{k_{-1}}{\overset{k_{+1}}{\rightleftarrows}} \text{Fe + Met80 + CL} \underset{k_{-2}}{\overset{k_{+2}}{\rightleftarrows}} \text{Fe-CL + Met80}$$

On the basis of the phenomenological Scheme 1, the observed rate constant can be determined from the following equation:

$$k_{obs} = \frac{k_{+1}k_{+2}[CL]}{k_{-1} + k_{+2}[CL]} + \frac{k_{-2}k_{-1}}{k_{-1} + k_{+2}[CL]} \quad (3)$$

where the parameters appearing in the equation correspond to those of Scheme 1. In eq 3, k_{obs} depends on [CL] as long as k_{+1} significantly differs from k_{-2}. Our data reveal that k_{obs} is independent of [CL] over the whole range investigated; this suggests that at least one of two conditions [(i) $k_{+1} \cong k_{-2} \approx 1.8$ s^{-1}, and/or (ii) $k_{+2}[CL] \gg k_{-1}$] must be satisfied [in case ii, the stability of the Fe−Met80 bond allows one to predict that $k_{-1} > 10k_{+1}$; this implies that at the lowest [CL] investigated, $k_{+2}(1.5 \times 10^{-5}) > 180$ s^{-1} and $k_{+2} > 1 \times 10^7$ M^{-1} s^{-1}, for $k_{+1} \cong 1.8$ s^{-1}]. At present, it is not possible to discriminate between conditions i and ii; however, the very similar rate constant values determined (Figures 6 and 7) provide support to condition i (i.e., $k_{+1} \cong k_{-2}$).

As shown in Figure 8, a signal change opposite in sign is observed when the cyt *c*−CL complex is mixed with NaCl. In agreement with measurements at equilibrium (Figure 3), data in the figure show that the salt induces dissociation of the cyt *c*−CL complex; the process is characterized by a very slow kinetic rate constant [$k_{obs} = (4.2 \pm 0.6) \times 10^{-3}$ s^{-1}] and requires several minutes to be completed. This very slow reactivity may be ascribed to either (i) an intrinsically very slow CL dissociation process or (ii) a high activation barrier for the tertiary changes leading to recovery of the Fe−Met80 axial bond. At present, there is no independent evidence supporting one option or the other, also because

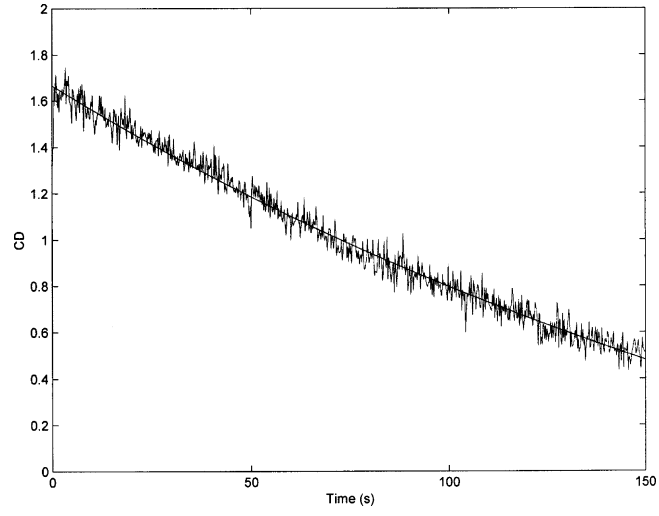

FIGURE 8: Kinetics of NaCl-induced complex dissociation. Kinetic progress curve of the dissociation of the CL−cyt *c* complex after addition of 400 mM NaCl. The complex consisted of 5 μM cyt *c* and 70 μM CL (concentration values in solution, after mixing). CD measurements were carried out at 416 nm. The solid line corresponds to nonlinear least-squares fitting of data to eq 1, employing the following values: $S_\infty = -0.86$, $\Delta S = 2.53$, and $k = 4.2 \times 10^{-3}$ s^{-1}. Other conditions were as described in the legend of Figure 1.

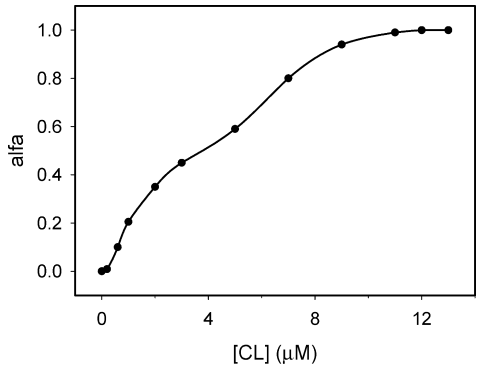

FIGURE 9: Peroxidase activity of CL-bound cyt c. Peroxidase activity of cyt c as a function of CL concentration, assessed by formation of tetraguaiacol. The protein concentration was 1 μM. The guaiacol concentration was 10 mM and the H_2O_2 concentration 1 mM. Data are reported as the fraction of the activity plateau value (see Results). Other conditions were as described in the legend of Figure 1.

CL binding to cyt c brings about a conformational change in the protein.

Peroxidase Activity of CL-Bound Cyt c. Upon binding to phospholipids, cyt c undergoes structural changes which facilitate the access of small molecules, such as hydrogen peroxide, into the heme site and induce peroxidase activity in the bound protein (*14*). In this study, the peroxidase activity of the CL-bound cyt c was measured by following the formation of orange-colored tetraguaiacol at low ionic strength after the addition of guaiacol and hydrogen peroxide to the solution containing cyt c and CL. As shown in Figure 9, peroxidase activity increases with CL concentration via a two-transition profile [similar to what is observed for CD data (Figure 2)]. Data were reported as fractions of the plateau value corresponding to a peroxidase activity of 160 nM s^{-1} (corresponding to a turnover number of 0.16 s^{-1}). Experiments carried out using Gdm-HCl as the denaturant agent showed a sigmoidal dependence of peroxidase activity on Gdm-HCl concentration with the maximal value (1400 nM s^{-1}) obtained with fully unfolded cyt c (data not shown). These results suggest that the phosholipid-bound protein is characterized by a less packed, but not denatured, non-native tertiary conformation. No peroxidase activity is shown by native cyt c.

DISCUSSION

In cell apoptosis, cyt c is released from the mitochondrial interface space into the cytosol (*27*). This critical event requires a decrease in the extent of the protein−CL interaction since this facilitates detachment of the protein from the membrane and its successive release into the cytosol (*13*). Thus, it appears clear that the strength of the cyt c−CL interaction plays an important role in the cell; it determines if cyt c will be retained in the intermembrane space carrying out its role in the respiratory chain or, conversely, released into the cytoplasm as in the apoptotic event.

Cyt c interacts with CL via two distinct sites, the A-site and the C-site, located on the protein surface and displaying different properties (*17, 18*). As described in detail in the introductory section, cyt c−CL interaction at the A-site is electrostatic in nature and is sensitive to ionic strength, while at the C-site, it is hydrophobic and implies H-bonding between residue N52 and the protonated phospholipid (*18, 28*). Around neutrality, ionic strength significantly affects protein−phospholipid binding; interactions that are electrostatic in nature (which imply CL binding at the A-site) are favored at low ionic strength, whereas interactions that are hydrophobic in nature (implying CL binding at the C-site) become predominant at high ionic strengths. Also, the negative surface density originated by CL concentration shifts the equilibrium toward the protonated form of the phospholipid, thus favoring cyt c−CL binding via the C-site (*18*).

Data in this paper show that at neutral pH the cyt c−CL binding process proceeds via two distinct transitions which are modulated by the phospholipid concentration (Figure 2). Since the cyt c−CL interaction via electrostatics is predominant at low ionic strengths and low phospholipid concentrations, we identify the A-site as the site involved in the first binding transition and indicate it as the high-affinity site for CL. The second transition, that occurring at a higher CL concentration, implies instead hydrophobic binding of CL to the protein via the C-site. Our data indicate that (i) saturation of both sites is necessary to achieve all the protein bound to CL (corresponding to the disappearance of the 416 nm dichroic signal at the end point of the second transition), (ii) the protein−CL interaction at the A-site is characterized by lower cooperativity ($n = 2$; see eq 2), and (iii) the protein−CL interaction at the C-site displays a steeper cooperative process, possibly ascribed to the conformational changes occurring in cyt c as CL binds at the C-site. In this respect, kinetic data suggest that the binding process possibly is characterized by a rate-limiting event (as shown by absorption and CD data). Clearly, this does not mean that the axial bond cleavage is the factor affecting the process (even though this possibility cannot be ruled out); it just suggests that a slow unimolecular structural change (with which cleavage of the axial bond is associated) likely is responsible for formation of the cyt c−CL complex. The existence of a rate-limiting step, represented by tertiary structural changes, is not new in cyt c folding−unfolding equilibria; a slow conformational change was observed in folding of cyt c, following the association of two protein fragments (*29*).

Also, the NaCl-induced complex dissociation is characterized by two distinct transitions. We identify the first transition as relative to dissociation of cyt c-bound CL from the A-site, due to the strong competitive action exerted by anions versus deprotonated CL; the transition observed at very high salt concentrations, instead, concerns the rupture of the cyt c−CL complex at the level of the C-site. In this last case, it is likely that CL dissociation is induced by unspecific binding of anions to cyt c. High anion concentrations were shown to influence cyt c conformation, inducing rearrangements of tertiary nature (*30, 31*); in this specific case, their action may weaken the cyt c−CL interaction at the level of the C-site, thus facilitating a cooperative dissociation of CL.

The finding that the C-site is implied in salt-induced complex dissociation may appear in contrast with an earlier study asserting that hydrophobic binding at the C-site is unaffected by ionic strength (*17*). However, in previous work, measurements were carried out in the presence of 180 mM sodium chloride as the maximum concentration; under such conditions, the second transition has not yet been observed in this study. On the other hand, the different CL:cyt c molar ratios used (23:1 vs 7:1) due to the different techniques that

were employed (requiring different cyt *c* concentrations for measurements) may represent another factor that is able to influence results.

Data on ATP-induced complex dissociation are in line with results discussed above. As evidenced by the CD spectrum of Figure 5, only approximately 50% of the complex is dissociated by the nucleotide. As described in the previous section, this represents the amount of protein interacting with CL at the high-affinity site. Thus, ATP competes with CL for only one site, identified here as the A-site in view of the fact that ATP binds to cyt *c* at a specific site composed of a cluster of charged residues (*32, 33*). Conversely, CL binding at the C-site does not appear to be influenced by ATP.

Unlike native cyt *c*, the CL-bound protein exhibits peroxidase activity characterized by a two-transition profile (see Figure 8). The accessibility of hydrogen peroxide to the iron site suggests that in CL-bound cyt *c* the heme crevice region is significantly altered and Met80 is displaced from the sixth coordination position of the heme iron. By comparing the maximum activity value of the CL-bound protein (160 nM s^{-1}) to that of the fully unfolded cyt *c* [1400 nM s^{-1}, a value in agreement with a previous finding (*34*)], we exclude any hypothesis of protein denaturation; thus, the CL-bound protein is characterized by a non-native partially unfolded tertiary conformation.

In conclusion, data in this paper provide new insights into the cyt *c*−CL interaction, by showing that (i) binding occurs via a cooperative two-transition process which implies a high-affinity site (the A-site) and a low-affinity site (the C-site), (ii) ionic strength exerts a strong influence on complex stability, inducing complex dissociation via two distinct transitions, the first implying the A-site and the other (which occurs at very high ionic strengths and is markedly cooperative) implying the C-site, (iii) ATP dissociates the complex, but its action appears to be limited to the A-site, (iv) upon (salt induced) complex dissociation, a high activation barrier is met by the protein for restoring the native Fe(III)−Met80 axial bond, and (v) CL-bound cyt *c* exhibits peroxidase activity. Thus, in the complex, the protein possesses a non-native, less packed (but not denatured) tertiary conformation. In line with earlier data, these results highlight the manifold functions of cyt *c* besides the well-known role played in the oxidative phosphorylation, shedding more light on the properties of the cyt *c*−CL complex, which is known to play a role in the execution of early stages of apoptosis. Results also support the view asserting that conformational changes in the tertiary nature of proteins (here, in cyt *c*) are a mechanism utilized by macromolecules to achieve structural diversity and, consequently, a diversity of functions.

REFERENCES

1. Moore, G. R., and Pettigrew, G. W. (1990) *Cytochromes c. Evolutionary, structural and physicochemical aspects*, Springer-Verlag, Heidelberg, Germany.
2. Pettigrew, G. W., and Moore, G. R. (1987) *Cytochromes c. Biological aspects*, Springer-Verlag, Heidelberg, Germany.
3. Bayir, H., Fadeel, B., Palladino, M. J., Witasp, E., Kurnikov, I. V., Tyurina, Y. Y., Tyurin, V. A., Amoscato, A. A., Jiang, J., Kochanek, P. M., DeKosky, S. T., Greenberger, J. S., Shvedova, A. A., and Kagan, V. E. (2006) Apoptotic interactions of cytochrome c: Redox flirting with anionic phospholipids within and outside of mitochondria. *Biochim. Biophys. Acta 1757*, 648–659.
4. Berezhna, S., Wohlrab, H., and Champion, P. M. (2003) Resonance Raman investigations of cytochrome c conformational change upon interactions with the membranes of intact and Ca^{2+} exposed mitochondria. *Biochemistry 42*, 6149–6158.
5. Liu, X., Kim, C. N., Yang, J., Jemmerson, R., and Wang, X. (1996) Induction of apoptotic program in cell-free extracts: Requirement for dATP and cytochrome c. *Cell 86*, 147–157.
6. Kluk, R. M., Bossy-Wetzel, E., Green, D. R., and Newmeyer, D. D. (1997) The release of cytochrome c from mitochondria: A primary site for Bc1-2 regulation of apoptosis. *Science 275*, 1132–1136.
7. Li, P., Nijhawan, D., Budihardjo, I., Srinivasula, S. M., Ahmad, M., Alnemri, E. S., and Wang, X. (1997) Cytochrome c and d-ATP dependent formation of Apaf-1/caspase-9 complex initiates an apoptotic protease cascade. *Cell 91*, 479–489.
8. Zou, H., Li, Y., Liu, X., and Wang, X. (1999) An Apaf-1 cytochrome c multimeric complex is a functional apoptosome that activates procaspase-9. *J. Biol. Chem. 274*, 11549–11556.
9. Purring-Koch, C., and McLendon, G. (2000) Cytochrome c binding to Apaf-1: The effects of dATP and ionic strength. *Proc. Natl. Acad. Sci. U.S.A. 97*, 11928–11931.
10. Jemmerson, R., Liu, J., Hausauer, D., Lam, K. P., Mondino, A., and Nelson, R. D. (1999) A conformational change in cytochrome c of apoptotic and necrotic cells is detected by monoclonal antibody binding and mimicked by association of the native antigen with synthetic phospholipid vesicles. *Biochemistry 38*, 3599–3609.
11. Quinn, P J., and Dawson, M. C. (1969) Interaction of cytochrome c and (^{14}C)carboxy-methylated cytochrome c with monolayers of phosphatidylcholine, phosphatidic acid and cardiolipin. *Biochem. J. 115*, 65–75.
12. Rytömaa, M., Mustonen, P., and Kinnunen, K. J. (1992) Reversible, non-ionic, and pH-dependent association of cytochrome c with cardiolipin-phosphatidylcholine liposomes. *J. Biol. Chem. 267*, 22243–22248.
13. Ott, M., Zhivotovsky, B., and Orrenius, S. (2007) Role of cardiolipin in cytochrome c release from mitochondria. *Cell Death Differ. 14*, 1243–1247.
14. Vladimirov, Y. A., Proskurnina, E. V., Izmailov, D. Y., Novikov, A. A., Brusnichkin, A. V., Osipov, A. N., and Kagan, V. E. (2006) Cardiolipin activates cytochrome c peroxidase activity since it facilitates H_2O_2 access to heme. *Biochemistry (Moscow, Russ. Fed.) 71*, 998–1005.
15. Kagan, V. E., Tyurin, V. A., Jiang, J., Tyurina, Y. Y., Ritov, V. B., Amoscato, A. A., Osipov, A. N., Belikova, N. A., Kapralov, A. A., Kini, V., Vlasova, I. I., Zhao, Q., Zou, M., Di, P., Svistunenko, D. A., Kurnikov, I. V., and Borisenko, G. G. (2005) Cytochrome c acts as a cardiolipin oxygenase required for release of proapoptotic factors. *Nat. Chem. Biol. 1*, 223–232.
16. Belikova, N. A., Vladimirov, Y. A., Osipov, A. N., Kapralov, A. A., Tyurin, V. A., Potapovich, M. V., Basova, L. V., Peterson, J., Kurnikov, I. V., and Kagan, V. E. (2006) Peroxidase activity and structural transitions of cytochrome c bound to cardiolipin-containing membranes. *Biochemistry 45*, 4998–5009.
17. Rytömaa, M., and Kinnunen, K. J. (1994) Evidence for two distinct acidic phospholipids-binding sites in cytochrome c. *J. Biol. Chem. 269*, 1770–1774.
18. Rytömaa, M., and Kinnunen, P. K. J. (1995) Reversibility of the binding of cytochrome c liposomes. Implications for lipid-protein interactions. *J. Biol. Chem. 270*, 3197–3202.
19. Tuominen, F. K., Wallace, C. J., and Kinnunen, P. K. J. (2002) Phospholipid-cytochrome c interaction: Evidence for the extended lipid anchorage. *J. Biol. Chem. 277*, 8822–8826.
20. Kawai, C., Prado, F. M., Nunes, G. L. C., Di Mascio, P., Carmona-Ribeiro, A. M., and Nantes, I. L. (2005) pH-dependent interaction of cytochrome c with mitochondrial mimetic membranes. The role of an array of positively charged amino acids. *J. Biol. Chem. 280*, 34709–34717.
21. Subuddhi, U., and Mishra, A. K. (2007) Micellization of bile salts in aqueous medium: A fluorescence study. *Colloids Surf., B 57*, 102–107.
22. Blauer, G., Sreerama, N., and Woody, R. (1993) Optical activity of hemoproteins in the Soret region. Circular dichroism of the undecapeptide of cytochrome c in aqueous solution. *Biochemistry 32*, 6674–6679.
23. Pielak, G. J., Oikawa, K., Mauk, A. G., Smith, M., and Kay, C. M. (1986) Elimination of the negative Soret Cotton effect of eukariotic cytochromes c by replacement of an invariant phenylalanine residue by site-directed mutagenesis. *J. Am. Chem. Soc. 108*, 2724–2727.
24. Santucci, R., and Ascoli, F. (1997) The Soret circular dichroism spectrum as a probe for the heme Fe(III)-Met(80) axial bond in horse cytochrome c. *J. Inorg. Biochem. 68*, 211–214.

25. Sinibaldi, F., Piro, M. C., Howes, B. D., Smulevich, G., Ascoli, F., and Santucci, R. (2003) Rupture of the H-bond linking two omega-loops induces the molten globule state at neutral pH in cytochrome c. *Biochemistry 42*, 7604–7610.
26. Touminen, E. K. J., Zhu, K., Wallace, C. J. A., Clark-Lewis, I., Craig, D. B., Rytömaa, M., and Kinnunen, P. K. J. (2001) ATP induces a conformational change in lipid-bound cytochrome c. *J. Biol. Chem. 276*, 19356–19361.
27. Green, D. R., and Reed, J. C. (1998) Mitochondria and apoptosis. *Science 281*, 1309–1312.
28. Kalanxhi, E., and Wallace, C. J. A. (2007) Cytochrome c impaled: Investigation of the extended lipid anchorage of a soluble protein to mitochondrial membrane models. *Biochem. J. 407*, 179–187.
29. De Sanctis, G., Ciaccio, C., Fasciglione, G. F., Fiorucci, L., Gioia, M., Marini, S., Sinibaldi, F., Santucci, R., and Coletta, M. (2004) Effect of axial coordination on kinetics of assembly and folding of the two halves of horse heart cytochrome c. *J. Biol. Chem. 279*, 52860–52868.
30. Sinibaldi, F., Howes, B. D., Smulevich, G., Ciaccio, C., Coletta, M., and Santucci, R. (2003) Anion concentration modulates conformation and stability of the molten globule of cytochrome c. *J. Biol. Inorg. Chem. 8*, 663–670.
31. Sinibaldi, F., Piro, M. C., Coletta, M., and Santucci, R. (2006) Salt-induced formation of the A-state of ferricytochrome c. Effect of the anion charge on protein structure. *FEBS J. 273*, 5347–5357.
32. Craig, D. B., and Wallace, C. J. A. (1993) ATP binding to cytochrome c diminishes electron flow in the mitochondrial respiratory pathway. *Protein Sci. 2*, 966–976.
33. Sinibaldi, F., Mei, G., Polticelli, M., Piro, M. C., Howes, B. D., Smulevich, G., Santucci, R., Ascoli, F., and Fiorucci, L. (2005) ATP specifically drives refolding of nonnative conformations of cytochrome *c*. *Protein Sci. 14*, 1049–1058.
34. Diederix, R. E., Ubbink, M., and Canters, G. W. (2002) Peroxidase Activity as a Tool for Studying the folding of c-type cytochromes. *Biochemistry 41*, 13067–13077.

BI800048V